ATL-INDET-2000-022
24/10/2000

ATLAS Internal Note
October 6, 2000

Determination of the ATLAS TRT straw tube active length

A. Lucotte[1)], V. A. Mitsou[1,2)], S. Mouraviev[1,3)]

Abstract

The performance of the TRT straw tubes in the regions near their ends is being discussed in this note. The counting rates and spectrum shapes are obtained by the irradiation of two straws with an X-ray source. Gas gain and energy resolution as a function of the position along the straw have been studied.

[1)]CERN, EP Division, CH-1211 Geneva 23, Switzerland
[2)]University of Athens, Physics Department, Nuclear and Particle Physics Section, Panepistimioupolis, GR-157 71 Athens, Greece
[3)]P.N. Lebedev Institute of Physics, Moscow, Russia

1 Introduction

Due to the presence of the end-plugs, different signal shapes and/or efficiency are generally expected to be observed at the extreme parts of the straws when compared to the middle part. The knowledge of the performance in these regions is important for a reliable representation of the detector response in the simulation package.

In order to study these effects, two low-eccentricity straws, assembled in the 4-plane prototype (type A) [1] were scanned with a highly collimated (0.5 mm) ^{55}Fe source. In fact, two sources were used to compensate for the low counting rate, irradiating in a direction perpendicular to the straw. The actual irradiated length of the straw, taking into account the geometry of the setup, was about 2 mm for a given position of the sources.

The spectra were obtained with the program `analysis.vi`, developed under BridgeVIEW$^{\mathrm{TM}}$, which reads out the CROSS module. This is capable of monitoring two straws simultaneously. The results described in the following sections concern one of the straws, but similar results were obtained with the other one.

2 Measurements and results

The outermost part of the straw was studied first. In this case, the crucial part of the straw is 'hidden' by the webs, therefore no divergence from the nominal operation of the straws neither was expected nor observed for the tested straws. This is evident from Fig. 1, while a more detailed view of this part of the straw can be found in Ref. [2].

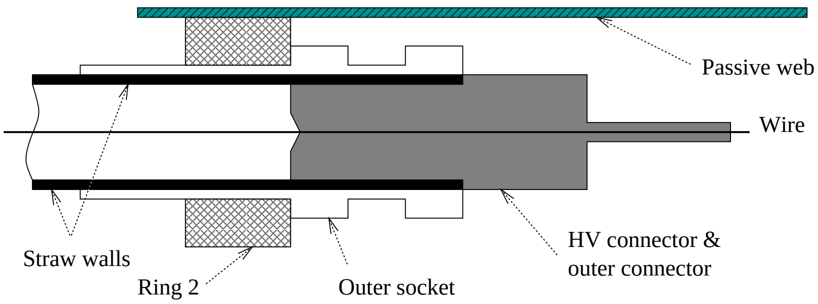

Figure 1: *Schematic view of the outermost part of a straw.*

At the inner end of the straws, however, the presence of part of the plastic socket inside the straw itself induces a significant reduction of the straw active length. Two straws of the 4-plane wheel, #0111[1] and #0121, were scanned with the X-ray source with a 1 mm step. As a point of reference ($x = 0$), the innermost edge of the straw was chosen, as shown in Fig. 2. Nevertheless, results are also shown in terms of the distance y from the surface of the inner ring, which is directly related to the detector geometry, as defined in the drawings.

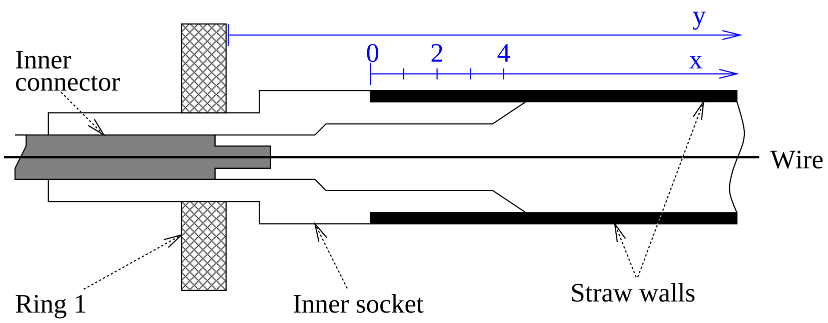

Figure 2: *Schematic view of the innermost part of a straw.*

According to Ref. [3], which describes the layout of the first 4-plane wheel, the distance of the straw edge from the inner ring is $y_0' = 2.5$ mm. But according to the final design for the inner end-piece [4], which is going to be used during the TRT assembly, this distance has a nominal value of $y_0 = 5.0$ mm. Since the part of the inner end-piece which is inside the straw has the same length for both layouts (4.5 mm), the results of this study are also valid for the current design. The distance y, which represents the distance between the measuring point and the inner ring, is therefore defined as $y \equiv x + y_0$.

The X-ray source spectra taken from various points along straw #0121 are shown in Fig. 3.

First of all, the straw was calibrated using the knowledge of the pedestal and the 5.9 keV X-ray peak as measured at the centre of the straw. In the following, the quoted values expressed in ADC channels are not pedestal-subtracted, unless otherwise stated.

The peak observed at low ADC channels, especially for the first five spectra, originates from events triggered by the other straw, which are therefore accumulated as ADC pedestals. This peak lies at 155 ADC channels with an r.m.s. of 3.5 ADC channels. The low-discrimination threshold, as defined for tracking purposes, is set at 200 eV, which corresponds to 172 ADC channels. This value is about five standard deviations above the pedestal, hence it excludes all triggers from noise. Moreover, as shown for the spectra for

[1]Straws are numbered according to the cell they belong to (cc: 1–96), the row (r: 1–8) and the layer (l: 1–4), i.e. as #$ccrl$.

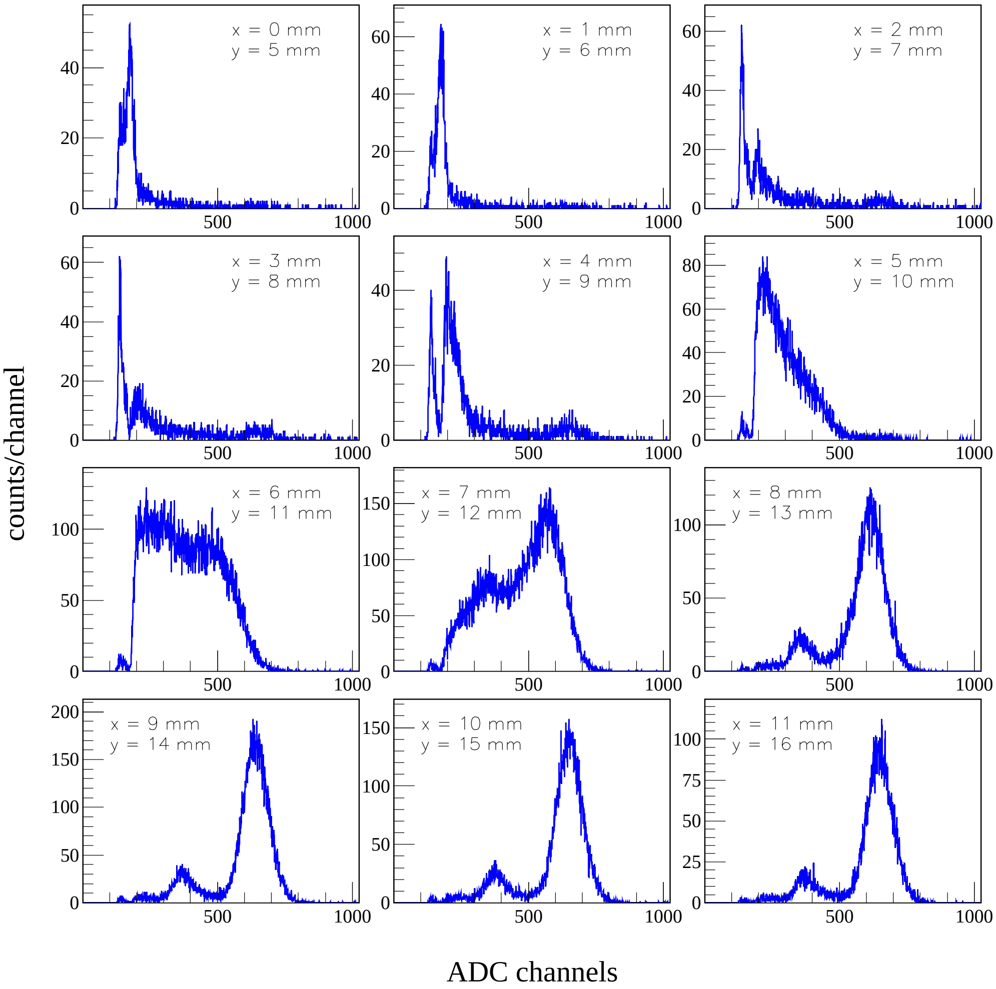

Figure 3: *X-ray source spectra taken at different positions along straw #0121. The peak at* $\sim$155 *ADC channels is the ADC's pedestal.*

$x \gtrsim 2$ mm, the low threshold lies between the pedestal and the rise of the actual signal spectrum, therefore by imposing a 200 eV threshold, all of the pedestal events are excluded without losing any substantial fraction of signal events.

A low but well-determined gas gain is observed for $x \lesssim 4$ mm due to the presence of the inner socket in the straw. This is made of plastic with an inner diameter of 3 mm. Moreover, the thickness of the plastic piece (~ 0.4 mm) results in a very low counting rate, corresponding to less than 1% of the one measured at the centre of the straw. Hence, this part of the straw ($x \lesssim 4$ mm) will not contribute at all to the tracking performance of the TRT system.

For $5 \lesssim x \lesssim 7$ mm, the counting rate increases significantly, as shown in Fig. 3, since the plastic piece is thinner and part of the irradiation zone covers the bare straw[2]. As far as the spectrum shape is concerned, it is distorted and shifted towards low energy values, which will affect considerably the operation of the straw with respect to the detection of high-energy transition radiation photons, but which nevertheless will provide tracking information of reasonable quality.

In the region $x \gtrsim 8$ mm, the expected typical spectrum is observed, although the gas gain and the energy resolution have not quite reached their optimal asymptotic values. These asymptotic values are reached for $x \gtrsim 9$ mm, where the counting rate saturates and the spectrum is restored to the shape observed at the centre of the straw.

The aforementioned observations in terms of efficiency, gas gain and resolution are summarised in Table 1 and Fig. 4. The counting rate is expressed as a percentage of the counting rate at the centre of the straw. Hence, the effects of the geometry and source radioactivity cancel. The counting rate was measured with a discriminated scaler thus avoiding counting as additional hits events accumulated as pedestals.

Table 1: *Signal amplitude A and resolution σ (in ADC channels), pedestal subtracted gas gain and counting rate, normalised to the values measured at the centre of the straw, and relative energy resolution, as a function of position along the straw.*

		Escape peak 2.7 keV	Main peak 5.9 keV			
x (mm)	y (mm)	A (σ) (ADC channels)		Gas gain (%)	σ/A'	Counting rate (%)
4	9	—	—	—	—	0.76
5	10	—	—	—	—	16.6
6	11	—	490 (77)	67.7	0.23	60.4
7	12	—	566 (62)	83.0	0.15	91.6
8	13	365 (45)	612 (52)	92.3	0.11	95.9
9	14	375 (41)	640 (46)	98.0	0.095	98.1
10	15	379 (39)	650 (47)	100.0	0.095	99.9
11	16	380 (39)	648 (46)	99.6	0.093	100.0

[2]The part of the plastic piece which is inside the straw has a length of 4.5 mm.

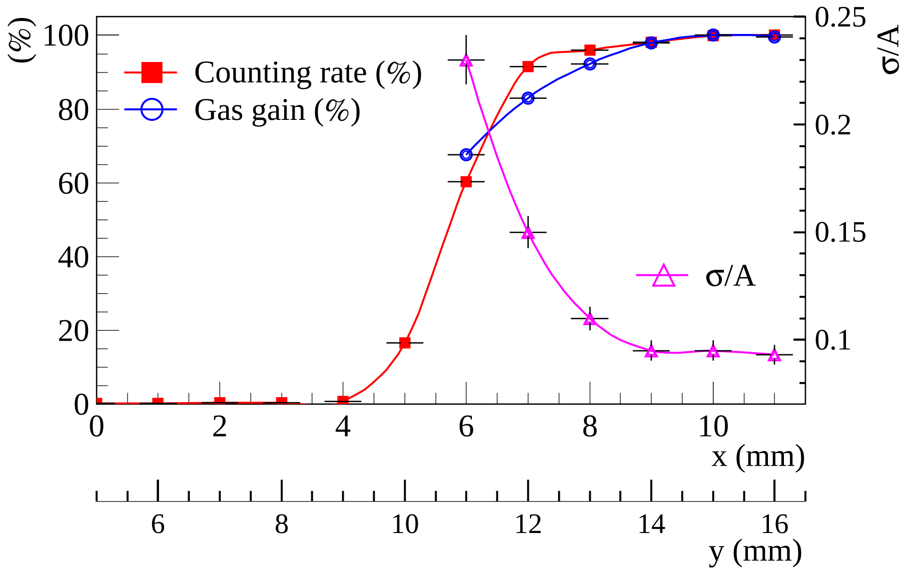

Figure 4: *Counting rate (closed squares), gas gain (circles) and energy resolution (triangles) as a function of the* ^{55}*Fe position along the straw.*

As gas gain, we define the pedestal-subtracted position of the 5.9 keV peak, normalised to the one observed at the centre of the straw. The 5.9 keV peak was used because it is determined with a better accuracy than the escape peak. Gas gain values are only quoted for $x \gtrsim 6$ mm, since the 5.9 keV peak can only be clearly identified in these spectra. For completeness, the evolution of the measured signal amplitude and resolution for $x \gtrsim 6$ mm is also shown in Table 1 for both escape and main peak. The accuracy achieved in the peak position determination is ± 2 ADC channels, i.e. $\pm 0.4\%$.

The energy resolution is also somewhat relevant to the performance of the detector, therefore it was also monitored. The ratio of the energy resolution over the pedestal-subtracted main peak position is also listed in Table 1. The relative resolution, σ/A, was determined with a precision of $\pm 5\%$.

For $x \gtrsim 10$ mm, the gas gain is stable and consistent with the one measured at the centre of the straw. The relative energy resolution, on the other hand, is also constant for $x \gtrsim 10$ mm and equal to $\sim 9\%$. Generally, the distortion of the electric field in a straw induced by the inner end-piece extends over $\sim$4.5 mm away from it. The efficiency becomes stable at a smaller distance, since it is mainly affected by the presence of the inner end-piece and only indirectly by the variation of the electric field.

Another profile of the spectra shapes and counting rates is given in Fig. 5. In this plot, the integrated number of events exceeding a given energy threshold is shown for various positions along the straw ($y \geq 10$ mm). Each curve is rescaled so that for a zero threshold it matches the measured counting rate (divided by the counting rate at the centre of the straw) in this position.

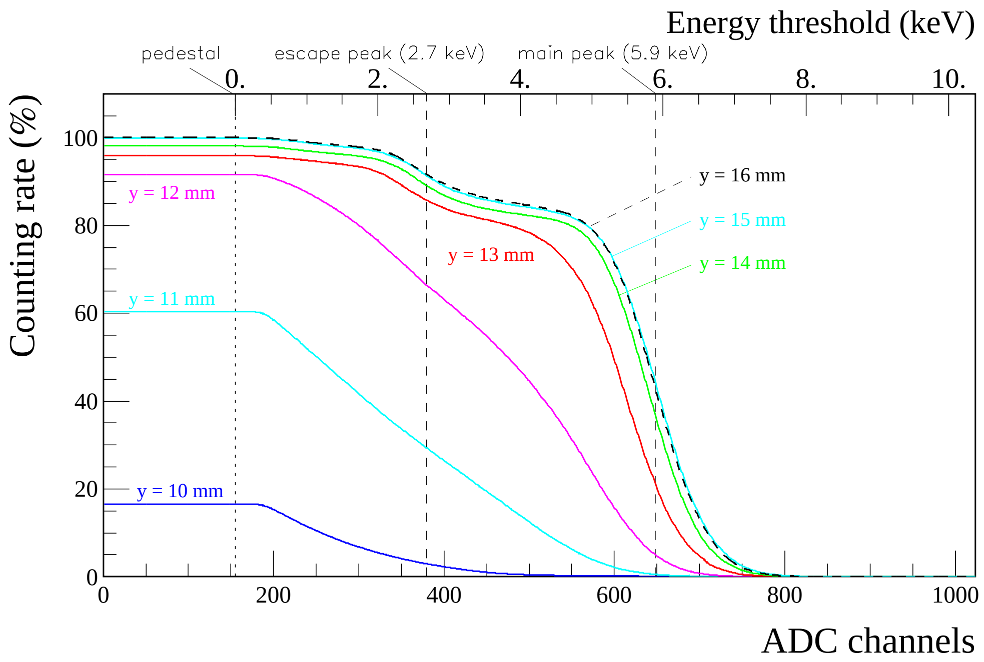

Figure 5: *Integrated number of events exceeding the threshold for different positions along the straw. The numbers have been normalised to the total number of events observed at the centre of the straw.*

3 Conclusions

The end-cap TRT straws demonstrate a uniform and stable performance —in terms of efficiency, gas gain and resolution— from a distance of $y \simeq 14$ mm from the outer surface of the inner support ring. Reliable information, especially in terms of low-threshold hits, nevertheless can be obtained even in the region $10 \lesssim y \lesssim 14$ mm: the detection efficiency and/or the gas gain are lower in this region, but it would be worth while to include them in the detector simulation.

As far as the outer radius is concerned, both the efficiency and the resolution are the same as in the centre of the straw at least up to 2 mm below ring 2. Dedicated measurements will be needed without webs to obtain a more accurate picture. The thin layer of plastic piece covering the straw ($\sim$3 mm thick) does not affect significantly the measured counting rate.

These results have by now been implemented in the overall simulation of the ATLAS TRT; their impact on the number of straw hits per track is visible, but the largest impact on these distributions since the TDR arises from the reduced dimensions of the outer support rings.

Acknowledgements

The authors would like to thank D. Froidevaux and F. Dittus for useful suggestions and many discussions. The work of V.A.M. was supported in part by the Greek State Scholarships Foundation (I.K.Y.).

References

[1] ATLAS Collaboration, Inner Detector Technical Design Report, vol. II, CERN/LHCC/97-17 (1997), Section 12.5.2.2.

[2] Drawing ATLITD 0018 (16.10.1998).

[3] Drawings ATLITD 0013 (16.10.1998) and ATLITD 0018 (16.10.1998).

[4] Drawings ATLITD 0021 (04.05.1999) and ATLITD 0023 (23.07.1999).